Features of plastic deformation and fracture of dispersion-strengthened V–Cr–Zr–W alloy depending on temperature of tension

Ivan A. Ditenberg, Ivan V. Smirnov, Konstantin V. Grinyaev, Yury P. Pinzhin, Alexander N. Tyumentsev, Anastasiya S. Tsverova, and Vyacheslav M. Chernov

Citation: AIP Conference Proceedings **1683**, 020042 (2015); doi: 10.1063/1.4932732
View online: http://dx.doi.org/10.1063/1.4932732
View Table of Contents: http://scitation.aip.org/content/aip/proceeding/aipcp/1683?ver=pdfcov
Published by the AIP Publishing

Features of Plastic Deformation and Fracture of Dispersion-Strengthened V–Cr–Zr–W Alloy Depending on Temperature of Tension

Ivan A. Ditenberg[1, 2, 3], Ivan V. Smirnov[1, 3, a)], Konstantin V. Grinyaev[1, 2, 3], Yury P. Pinzhin[1, 2], Alexander N. Tyumentsev[1, 2, 3], Anastasiya S. Tsverova[1], and Vyacheslav M. Chernov[4]

[1] *National Research Tomsk State University, Tomsk, 634050 Russia*
[2] *Institute of Strength Physics and Materials Science SB RAS, Tomsk, 634055 Russia*
[3] *Siberian Physical-Technical Institute, Tomsk, 634050 Russia*
[4] *A.A. Bochvar High Technology Research Institute of Inorganic Materials, Moscow, 123098 Russia*

[a)] Corresponding author: smirnov_iv@bk.ru

Abstract. Influence of tension temperature on features of plastic deformation and fracture of V–4.23Cr–1.69Zr–7.56W alloy was investigated by scanning and transmission electron microscopy. It is shown that temperature increase leads to activation of the recovery processes, which manifests in the coarsening of microstructure elements, reducing the dislocation density, relaxation of continuous misorientations.

INTRODUCTION

To date, low activation vanadium-based alloys are considered as promising construction materials for nuclear power plants of new generation [1, 2]. The efficiency of dispersion strengthening of modern vanadium alloys, mostly presented by V–4Ti–4Cr-system, is significantly limited by both relatively low values of interstitial elements concentration and, consequently, low volume fraction of second phase particles, and by low thermal stability of these particles [3–7]. In order to improve the performance properties of these alloys the works are conducted to optimize their elemental composition and to develop methods of modification of structural-phase states.

In [5–7] vanadium alloys of new V–Cr–Zr–W-system were proposed, which processing by methods of thermomechanical treatment (TMT) and chemical-heat treatment (CHT) provides a significant, as compared with V–4Ti–4Cr alloys, raising in recrystallization temperature and increase in high-temperature strength characteristics while maintaining acceptable levels of low temperature plasticity.

In current paper the study of features of plastic deformation and fracture of V–Cr–Zr–W–system alloy, subject to tension temperature was conducted by transmission and scanning electron microscopy.

EXPERIMENTAL MATERIALS AND PROCEDURES

The study was conducted with the use of V–4.23Cr–1.69Zr–7.56W (wt %) alloy after complex processing, comprising TMT stages for dispersing the initial coarse phase [6] and the oxygen doping in the CHT process [7]. Mechanical testing of samples by active tension were performed at temperatures of 20, 800, 900 and 1000°C in Polanyi tensile testing machine with a movable lower grip. Specimen tension direction (TD) coincides with the direction of rolling (RD) during TMT. Features of plastic deformation were studied in the area of maximum deformation near fracture formation of specimens after tension. Studies of surface relief and features of fracture were carried out using a scanning electron-ion microscope Quanta 200 3D (30 kV). Orientation maps were obtained

Advanced Materials with Hierarchical Structure for New Technologies and Reliable Structures
AIP Conf. Proc. 1683, 020042-1–020042-4; doi: 10.1063/1.4932732

by Electron BackScatter Difraction (EBSD), modes and conditions of this process are described in [8]. Study of thin foils was carried out with the use of transmission electron microscope Philips CM30 (300 kV). Methods of samples preparation for investigation by transmission and scanning electron microscopy and the methods used to study and analyze the microstructure were presented in [8].

RESULTS AND DISCUSSION

After combined treatment (TMT + CHT) and stabilizing annealing at 1100°C the structural state of investigated alloy is characterized by high heterogeneity of grain structure (Fig. 1a) elongated in rolling direction (RD). There are three main fractions of grains: large, 10–30 μm in width, reaching a length of 50 μm or more microns; medium, width of which is 5–15 μm and length is 10–50 μm; small crystallites with close to equiaxial shape up to 5 μm in size. Most of the grains on orientation maps have a gradient color that indicates the presence of continuous misorientations inside. Second phase is represented by particles based on ZrO_2 with minor concentrations of carbon and nitrogen [5, 7]. Three fractions of particles were revealed (Figs. 1b and 1c): coarse particles of almost spherical shape, more than 500 nm in size; particles of similar shape with dimensions of 50–300 nm; nanosized particles of 3–10 nm in size. The important point is that the large particles and the middle fraction are practically lack on grain boundaries, while the fine particles up to 10 nm are uniformly distributed over the material volume, fixing the dislocation structure (Fig. 1c). Scalar dislocation density reaches $(3–5)\times 10^{10}$ cm^{-2}.

Grain structure on orientation maps obtained after tension at 20 C (Fig. 2a), as in the initial state (Fig. 1a), consists of three major fractions. Meanwhile there is intensification of fragmentation within large and medium grains, in which the density of discrete-type low-angle boundaries increases, and more gradient color, compared to the initial (Fig. 1a), inside grains indicates an increase in continuous-type misorientations. Grains are characterized mainly by the form elongated in the tension direction (TD).

The grain structure after tension at temperatures of 800 and 900°C (Fig. 2b) is characterized by more developed fragmentation of large grains, resulting in an increase in the number of grains of small and medium fractions. In our opinion, this is due to the relaxation of high continuous misorientations into discrete boundaries during fragmentation of large grains, as also evidenced by a decrease or lack of gradient color in fragments formed (Fig. 2b). Gradient color increases within the remaining large grains.

Significant changes in microstructure are observed after tension at 1000°C (Fig. 2c). Large fraction grains lack on orientation maps, while the bulk of the material is represented by grains of medium fraction practically without gradient color. Small grains (less than 5 microns in size) are generally observed in the form of clusters elongated in the tension direction, which are a result of intense fragmentation of the initial grains of medium and large fractions.

Transmission electron microscopy study showed, that a common feature of plastic deformation of V–Zr–Cr–W alloy under tension at temperatures of 20–1000°C is its localization mainly in the fine fraction grains (5 μm) with formation of microbands (Fig. 3) extending in the rolling direction of the samples at TMT, almost parallel to the rolling plane (RP). At the same time, depending on the tension temperature the bands above differ in size and dislocations density.

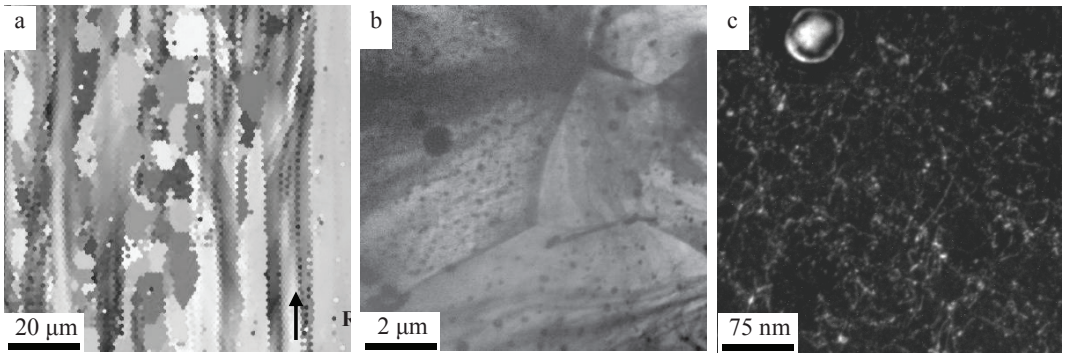

FIGURE 1. Microstructure of the experimental specimen following combined treatment. Orientation maps (a), bright-field (b) and dark-field (c) electron microscopy images. Scanning electron microscopy, EBSD method (a); transmission electron microscopy (b, c)

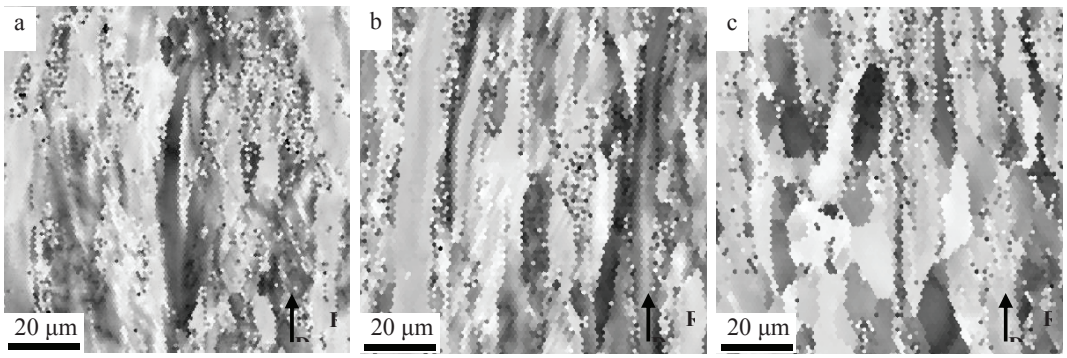

FIGURE 2. Orientation maps of microstructure of experimental specimens after subsequent plastic deformation at temperatures 20 (a), 800 (b) and 1000°C (c). Scanning electron microscopy (EBSD method)

After tension at 20°C microband structure is represented by bands 0.2–0.3 μm in width (Fig. 3a), which form the packs up to a few microns in thick. These bands are divided inside in the longitudinal direction with transverse boundaries on subgrains with length of 1 μm. The scalar density of dislocations within these fragments reaches $(1–1.2)\times10^{11}$ cm^{-2}.

Deformation temperature increase up to 800°C results in increase in bands width up to 0.4–0.8 μm (Fig. 3b). The longitudinal dimensions of the bands within the subgrains are also increased, reaching 0.5–1 μm. Scalar dislocation density is reduced to $(0.4–1)\times10^{11}$ cm^{-2}. At deformation temperature 900°C there is a significant increase in fraction of bands of approximately 1 μm in width, in which dislocation density substantially reduces to $(3–5)\times10^{10}$ cm^{-2}.

After tension at temperature of 1000°C width of bands is practically unchanged, but the longitudinal size of subgrains substantially (up to several microns) increase (Fig. 3c). Scalar dislocation density reaches minimum values $(1–5)\times10^{10}$ cm^{-2}.

It should be noted that during the investigation no special features were revealed, which could indicate the influence of tension temperature on both processes of coagulation of second phase particles and character of the spatial distribution of fine-disperse (10 nm) particles in microbands formed as a result of localization of plastic deformation.

Tension fractographs are presented on Fig. 4. At 20°C in fracture area (Fig. 4a) both signs of brittle and ductile fracture are observed. Ductile type of fracture (Figs. 4b and 4c) is predominantly characteristic for high temperatures (800–1000°C). It was found that test temperature increase from 800 to 1000°C leads to a coarsening of fracture structure and increase in cell size of pit relief from (1–3) μm to (3–10) μm (Figs. 4b and 4c). Main feature of fracture at high (800–1000°C) temperatures is an intensive formation and increase in size of cracks on the side surfaces which viscously open in the direction of tension.

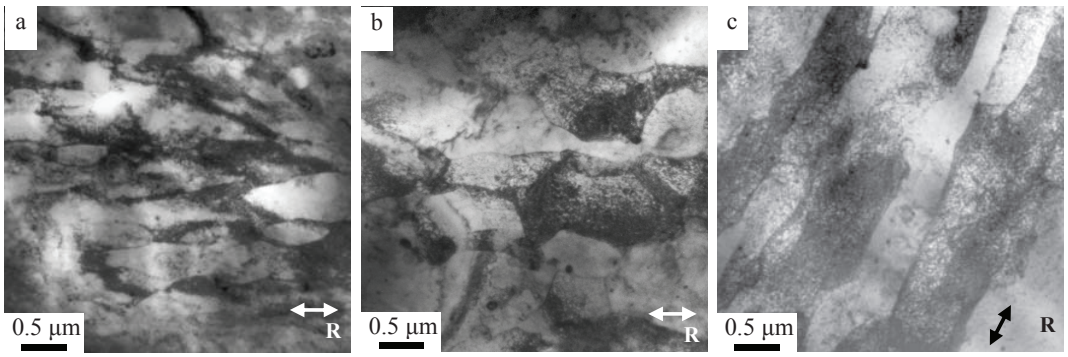

FIGURE 3. Bright-field electron microscopy images of microstructure of V–Zr–Cr–W alloy after deformation at temperatures 20 (a), 800 (b) and 1000°C (c). Transmission electron microscopy

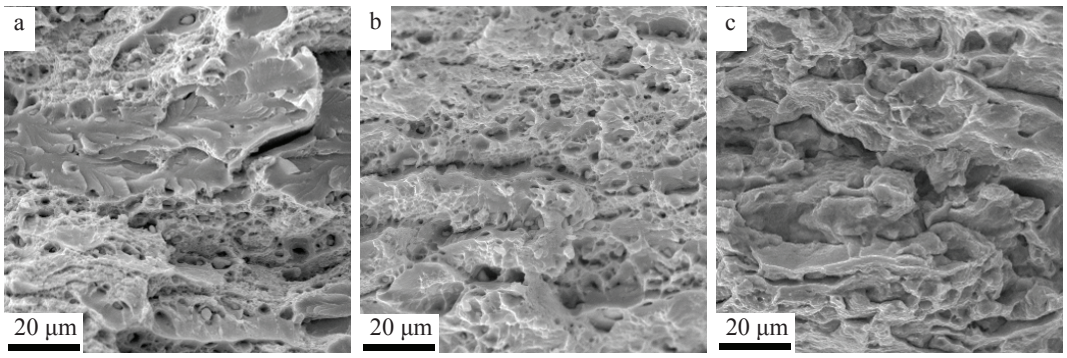

FIGURE 4. Fracture relief of V–Zr–Cr–W alloy samples after tension at temperatures 20 (a), 800 (b) and 1000°C (c). Scanning electron microscopy

SUMMARY

Investigation has shown that in conditions of active tension the result of plastic deformation localization near fracture formation area is the intensification of the processes of fragmentation of crystal lattice, developing at different scale levels. Tension temperature increase activates the recovery processes, which manifests in the coarsening of elements of grain and subgrain structure, decrease in dislocation density, relaxation of continuous-type misorientations, and also leads to coarsening of fracture area structure and increase in size of pit relief cells. Lack of coagulation and redistribution of fine second phase particles under tension at high (800–1000°C) temperatures was found.

ACKNOWLEDGMENTS

The work was conducted within the framework of the Program for Fundamental Scientific Research of State Academies of Sciences for 2013–2020 (deformation and thermal treatments, tension tests) at partial financial support of Tomsk State University Competitiveness Improvement Program (transmission and scanning electron microscopy). Investigation was carried out using the equipment of the Tomsk State University.

REFERENCES

1. S. J. Zinkle, A. Möslang, T. Muroga, and H. Tanigawa, Nucl. Fusion **53**, 104024 (2013).
2. T. Muroga, J. M. Chen, V. M. Chernov, R. J. Kurtz, and M. Le Flem, J. Nucl. Mater. **455**, 263 (2014).
3. A. N. Tyumentsev, A. D. Korotaev, Yu.P. Pinzhin, I. A. Ditenberg, S. V. Litovchenko, Ya. V. Shuba, N. V. Shevchenko, V. A. Drobishev, M. M. Potapenko, and V. M. Chernov, J. Nucl. Mater. **329–333**, 429–433 (2004).
4. A. N. Tyumentsev, I. A. Ditenberg, K. V. Grinyaev, V. M. Chernov, and M. M. Potapenko, J. Nucl. Mater. **413**, 103 (2011).
5. V. M. Chernov, M. M. Potapenko, V. A. Drobishev, M. V. Kravtsova, A. N. Tyumentsev, S. V. Ovchinnikov, I. A. Ditenberg, Yu. P. Pinzhin, A. D. Korotaev, I. V. Smirnov, K. V. Grinyaev, and I. I. Sukhanov, Nucl. Mater. Energ. (*accepted for publication*).
6. A. N. Tyumentsev, I. A. Ditenberg, K. V. Grinyaev, I. V. Smirnov, V. M. Chernov, and M. M. Potapenko, AIP Conf. Proc. **1623**, 643 (2014).
7. N. Tyumentsev, A. D. Korotaev, Yu. P. Pinzhin, S. V. Ovchinnikov, I. A. Ditenberg, A. K. Shikov, M. M. Potapenko, and V. M. Chernov, J. Nucl. Mater. **367–370**, 853 (2007).
8. A. Ditenberg, K. V. Grinyaev, A. N. Tyumentsev, I. V. Smirnov, V. M. Chernov, and M. M. Potapenko, Russ. Phys. J. **58**, 205 (2015).